## ORIGINAL RESEARCH

# Platelet-Mimicking Nanosponges for Functional Reversal of Antiplatelet Agents

Junchao Xu*, Na Yan*, Chunling Wang, Chao Gao, Xuexiang Han, Chengzhi Yang, Jiaqi Xu, Kun Wang, Michael J. Mitchell, Yinlong Zhang, Guangjun Nie

**BACKGROUND:** During long-term antiplatelet agents (APAs) administration, patients with thrombotic diseases take a fairly high risk of life-threatening bleeding, especially when in need of urgent surgery. Rapid functional reversal of APAs remains an issue yet to be efficiently resolved by far due to the lack of any specific reversal agent in the clinic, which greatly restricts the use of APAs.

**METHODS:** Flow cytometry analysis was first applied to assess the dose-dependent reversal activity of platelet-mimicking perfluorocarbon-based nanosponges (PLT-PFCs) toward ticagrelor. The tail bleeding time of mice treated with APAs followed by PLT-PFCs was recorded at different time points, along with corresponding pharmacokinetic analysis of ticagrelor and tirofiban. A hemorrhagic transformation model was established in experimental stroke mice with thrombolytic/antiplatelet therapy. Magnetic resonance imaging was subsequently applied to observe hemorrhage and thrombosis in vivo. Further evaluation of the spontaneous clot formation activity of PLT-PFCs was achieved by clot retraction assay in vitro.

**RESULTS:** PLT-PFCs potently reversed the antiplatelet effect of APAs by competitively binding with APAs. PLT-PFCs showed high binding affinity comparable to fresh platelets in vitro with first-line APAs, ticagrelor and tirofiban, and efficiently reversed their function in both tail bleeding and postischemic-reperfusion models. Moreover, the deficiency of platelet intrinsic thrombotic activity diminished the risk of thrombogenesis.

**CONCLUSIONS:** This study demonstrated the safety and effectiveness of platelet-mimicking nanosponges in ameliorating the bleeding risk of different APAs, which offers a promising strategy for the management of bleeding complications induced by antiplatelet therapy.

**GRAPHIC ABSTRACT:** A graphic abstract is available for this article.

**Key Words:** antiplatelet agents ■ antithrombotic reversal agents ■ bio-inspired engineering ■ hemorrhage ■ platelet transfusion ■ theranostic nanomedicine

---

### Meet the First Author, see p 253

Thrombotic events, mainly ischemic stroke and acute myocardial infarction, are the leading causes of death worldwide, with growing morbidity and mortality coinciding with the rapidly growing aging population.[1,2] Due to the dominant role of activated platelets in the formation of pathological thrombosis, controllable platelet inhibition is regarded as a central strategy against thrombogenesis.[3] To date, the clinical usage of antiplatelet agents (APAs), mainly aspirin, P2Y$_{12}$ inhibitors (eg, clopidogrel, ticagrelor, cangrelor, and prasugrel), GP (glycoprotein) IIb/IIIa inhibitors (eg, tirofiban, eptifibatide, and abciximab), and PAR (protease-activated receptor) inhibitors,

---

## Novelty and Significance

### What Is Known?

- There is a need for functional reversal of antiplatelet agents in patients with long-term usage to decrease high bleeding risk particularly in cases of urgent need of surgery.
- Platelet transfusion is either inadequate to reverse the effect of antiplatelet agents or excessive to cause thrombus.

### What New Information Does This Article Contribute?

- This study outlines a platelet-mimicking nanosponge strategy for the functional reversal of antiplatelet agents without thrombogenic potential.
- Unlike other prohemostatic strategies, nanosponges achieved functional reversal by competitively binding with antiplatelet drugs, thus avoid compromising urgent revascularization.
- Unlike platelet transfusion, nanosponges cannot induce clot retraction due to its inactive perfluorocarbon core.

Long-term antiplatelet administration can cause increased bleeding risk. Patients with acute hemorrhage, or in need of invasive interventions, require urgent reversal of antiplatelet drugs. Platelet transfusion can be inadequate to reverse the effect of certain antiplatelet agents, or can be excessive to elicit thrombogenesis. This study demonstrates the feasibility of a platelet-mimicking nanosponge strategy capable of functional reversal of antiplatelet drugs. Unlike other prohemostatic strategies, nanosponges achieved functional reversal by competitively binding with antiplatelet drugs, thus not compromising urgent revascularization. Moreover, nanosponges themselves do not induce clot retraction like normal platelets due to the inactive perfluorocarbon core, while their adhesion behavior was conserved. In the future, the nanosponges may serve as a broad-spectrum reversal agent for platelet membrane receptor inhibitors.

## Nonstandard Abbreviations and Acronyms

| | |
|---|---|
| **APA** | antiplatelet agent |
| **AUC** | area under the curve |
| **PLT-PFC** | platelet-mimicking perfluorocarbon-based nanosponge |
| **PNV** | platelet nanovesicles |

has become one of the main strategies in the treatment of thrombosis-associated diseases.[4] During the medication period, life-threatening bleeding events, in particular intracranial hemorrhage, stand a fair chance of occurrence.[4,5] The effective maintenance of platelet inhibition by APAs, so as to prevent fatal thrombotic events while maintaining adequate hemostatic activity, remains an unmet medical challenge.[6,7] Patients in urgent need of surgery, such as coronary-artery bypass graft, are usually instructed to stop medication for up to 3 to 10 days until the APAs are fully cleared from the blood circulation, allowing platelet function to gradually return to a normal state.[8,9] Standard platelet transfusion is expected to restore platelet function in many clinical settings.[10] However, only modest efficiency has been achieved in the recovery of hemostatic function by platelet transfusion, only to bring more unpredictable imbalance between thrombotic and bleeding risk.[11–13] Upon platelet transfusion, excessive free reversible APAs or their active metabolites efficiently occupy their binding targets on the dose-limited fresh platelets, leading to ineffective platelet function reversal.[14] In contrast, excessive

doses of transfused platelets can bring more severe side effects, including excessive platelet activation with an enhanced thrombogenic milieu in vivo.[11,12,15]

Several alternatives have been attempted to solve the bleeding issue. A highly specific antibody fragment, Bentracimab, potently neutralizes ticagrelor and its active metabolite in blood.[16] Despite its great potency, its high specificity for ticagrelor and high cost of antibody production may limit its potential applicability for functional reversal of antiplatelet therapy. Therefore, the development of universal and accessible APA reversal agents is greatly needed.

Inspired by the mechanisms of action of APAs and the successful application of platelet-based biomimetic nanoparticles,[17–19] we hypothesized that platelet membrane nanosponges may prove to be advantageous as a broad-spectrum APA reversal agent. To this end, we constructed a platelet-mimicking perfluorocarbon-based nanosponge (PLT-PFC) consisting of a platelet membrane as the shell and biocompatible perfluorocarbon (PFC) as the inner core. Herein, we demonstrated this formulation's feasibility as a reversal agent for binding and neutralizing different APAs (ie, ticagrelor and tirofiban), via a high affinity competition for the specific interaction of APAs with their corresponding receptors. By displaying platelet membrane receptors, such as $P2Y_{12}$ and GPIIb/IIIa receptors, on their surface, the platelet nanosponge is expected to mimic natural platelets and thus binds with APAs targeting various platelet receptors that would otherwise inhibit circulating endogenous platelets (Figure 1). We found that PLT-PFCs significantly decreased the concentration of free APAs in the plasma and recovered platelet aggregation
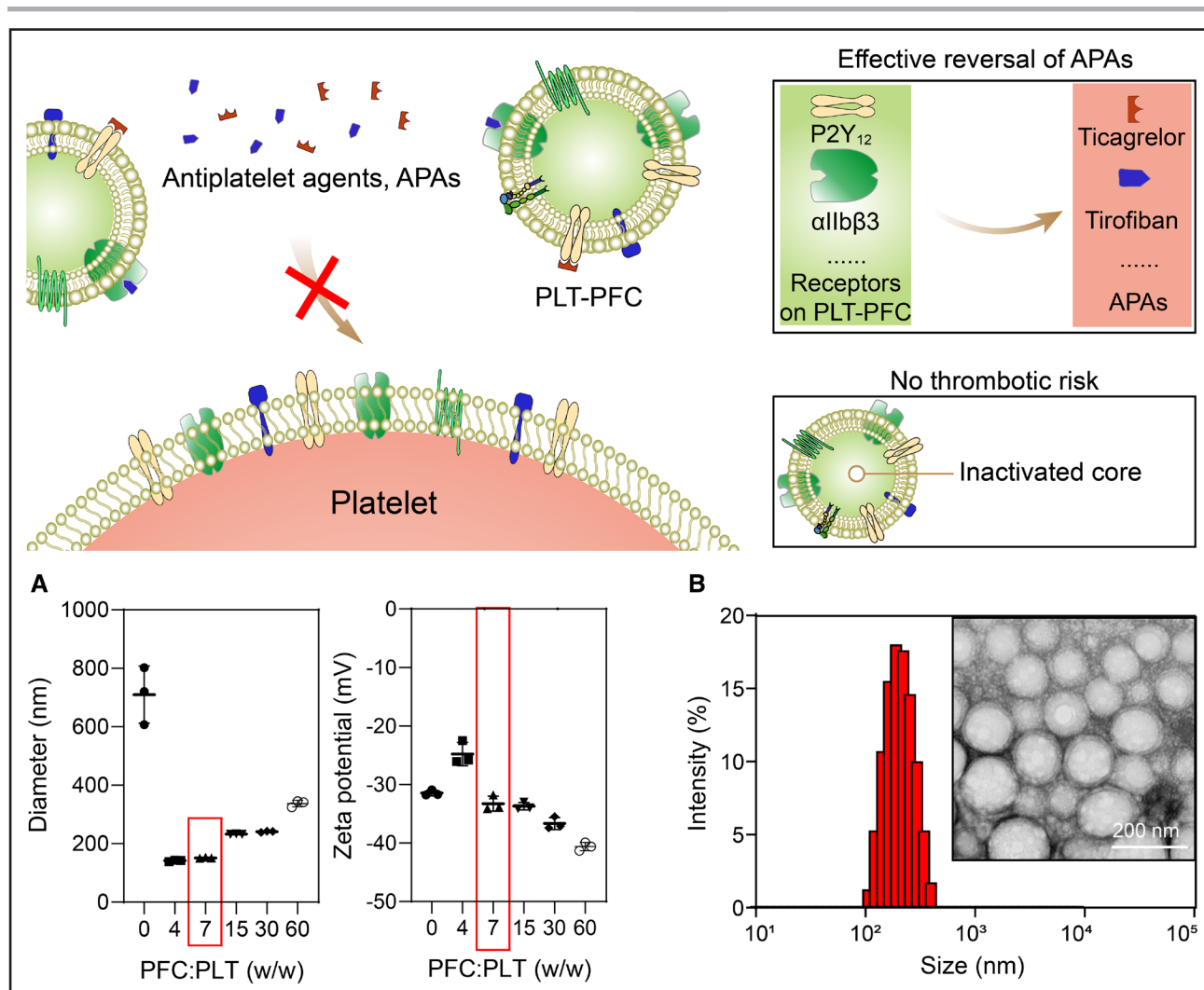
**Figure 1. Preparation and physicochemical characterization of platelet-mimicking perfluorocarbon-based nanosponges (PLT-PFCs).**

Schematic illustration of PLT-PFCs as universal reversal agents of antiplatelet agents (APAs). PLT-PFCs competitively bind to APAs at their corresponding specific platelet membrane receptors to prevent the bleeding risk, while the substitution of the intraplatelet matrix with an inactive PFC core diminishes the thrombotic risk. **A**, Diameter and zeta potential of PLT-PFCs at the indicated PFC to platelet membrane ratios 7:1 (PFC:platelet, w/w) was the optimal ratio (indicated by the red frame), with an appropriate size and zeta potential (n=3). **B**, Average hydrodynamic size of PLT-PFCs at around 150 nm (n=3) and their morphology (transmission electron microscopy). Scale bar = 200 nm.

in the ticagrelor-spiked human plasma, thereby potently restoring platelet function and normalizing hemostasis both in binding affinity assays and in animal models of tail bleeding and stroke, as well as an experimental stroke model followed by hemorrhagic transformation induced by thrombolysis and antiplatelet therapy in vivo. Clot retraction assays and coagulation tests suggest that PLT-PFC transfusion presents a low risk of thrombosis induction in comparison with its 20% equivalent dosage of traditional platelet transfusion. All these results demonstrate that PLT-PFC transfusion may be used as a broad-spectrum reversal strategy of APAs with acceptable biosafety. PLT-PFC transfusion may provide a practical strategy to satisfy the urgent need for APA reversal agents, thus overcoming the obstacles encountered by the current practice of platelet transfusion.

## METHODS

### Data Availability

The data that support the findings of this study are available from the corresponding author upon reasonable request.

A detailed methods section is provided in the Supplemental Material. Please see the Major Resources Table in the Supplemental Material.

## RESULTS

### Preparation and Physicochemical Characterization of PLT-PFCs

First, we applied PFC as the biocompatible core material to stabilize cellular membranes, as described in previous

reports.[20,21] Platelet membrane was coated onto the surface of PFC to form uniform biomimetic nanosponges (PLT-PFCs) by ultrasonic emulsification and coextrusion. To optimize the coating efficiency, different volumes of core nanoparticles with the fixed concentration of 1 mg/mL and platelet membranes from $1\times10^8$ platelets were co-incubated. As shown in Table S1, we obtained ~3.12±1.11 mg platelet membranes per $1\times10^8$ platelets. We next evaluated the size distribution and zeta potential of PLT-PFCs fabricated with different ratios of PFC and platelet membrane. As PFC increased, the particle size increased accordingly, while the zeta potential decreased, which is similar to the observations in previous studies on cell membrane-derived nanoparticles.[20] At a ratio of ~7:1 (PFC:platelet, w/w), the zeta potential of PLT-PFCs became close to the platelet membrane at ~34 mV, indicating that the platelet membrane was almost completely coated onto the PFC core (Figure 1A). In this case, the average hydrodynamic size of PLT-PFCs was ~150 nm (Figure 1B), which has been reported to be a suitable size for the desired pharmacokinetic properties, including the prevention of rapid renal clearance or reticuloendothelial system capture.[22] Under transmission electron microscopy, PLT-PFCs presented a typical core-shell nanostructure morphology, with a diameter of ~150 nm. The size distribution profile of the resulting PLT-PFCs remained highly stable, while the pharmacological effects were also retained after 6 months of storage at −80 °C (Figure S1). We also characterized the size and zeta potential of all the drug formulations used in this study by dynamic laser scattering (Table S2).

## Functional Protein Characterization of PLT-PFCs

Next, we conducted nano-flow cytometry to identify the key functional receptors, $P2Y_{12}$ and αIIb/β3 (ie, GPIIb/IIIa) receptors (Figure 2A) with a gating strategy as shown in Figure S2. Apart from $P2Y_{12}$ and αIIbβ3 receptors, we next identified the existence of other main platelet membrane receptors including GPVI, GPIbα, and CD49b receptors on the surface of PLT-PFCs (Figure S3). Meanwhile, the intracellular domain of CD49b was not readily labeled as its extracellular domain by corresponding antibodies, indicating the right-side-out orientation of the PLT-PFCs. Next, we tested the functionality of these receptors by incubating Cy5-labeled PLT-PFCs with fibrinogen, von Willebrand factor, or collagen pre-coated microplates (Figure S4). In parallel, excessive antibodies were also preincubated with PLT-PFCs to block CD61, GPIbα, or GPVI. All these antibodies could partially, instead of completely, inhibit the binding affinity of PLT-PFCs to fibrinogen, von Willebrand factor, or collagen. In addition, we used the PAR4 N-terminal antibody to characterize the conformational change of the PAR4 receptor after its N-terminal cleavage by thrombin. These characterization results indicated that PLT-PFCs retained most of the important receptors expressed on platelets and their functions. We next examined the overall protein distribution of PLT-PFCs, platelet nanovesicles (PNV), and whole platelet protein lysates by SDS-PAGE. No statistical differences in protein profile were observed between the PLT-PFC and PNV groups (Figure 2B). To characterize the overall surface receptors retained on PLT-PFCs, we carried out differential analysis of protein expression between PLT-PFCs and platelets, according to the proteomics results. Volcano plots (Figure 2C and 2D) visualized the significant changes in cytoplasmic and membrane proteins of PLT-PFCs and platelets. In general, up to 86.2% of platelet cytoplasmic proteins decreased in PLT-PFCs, while 82.3% of platelet membrane proteins were retained in the PLT-PFC group. These results further demonstrated the retention and enrichment of platelet membrane proteins, which was consistent with previous studies on biomimetic membrane-cloaking nanoparticles.[17,23] However, PLT-PFCs neither cleared all cytoplasmic proteins nor retained all membrane proteins.

Western blot analysis further confirmed the preservation of key surface receptors, including CD41, CD61, and $P2Y_{12}$, together with the loss of the intracellular housekeeping protein, GAPDH (glyceraldehyde phosphate dehydrogenase) in the PLT-PFC and PNV protein lanes (Figure 2E) semiquantified and analyzed from the gel blots (Figure S5). These results together demonstrate the preservation of membrane receptors on the synthetic PLT-PFCs and the removal of intracellular proteins. Nano-flow cytometry results indicated the PLT-PFC surface has a small proportion of phosphatidylserine (Figure S6). Although the PS surface is thought to provide a thrombogenic surface in local thrombosis,[24] the proportion of PS surface was limited with negligible thrombotic potential, which was proven by further results of platelet aggregation rate, bleeding time, and coagulation indicators.

## In Vitro Binding Affinity of PLT-PFCs to APAs and Platelet Function Reversal

To evaluate the binding affinity of PLT-PFCs to APAs, we determined the equilibrium association constant (Ka) and equilibrium dissociation constant (Kd) by isothermal titration calorimetry and microscale thermophoresis analysis, respectively (Figure 3A). The binding affinity of PLT-PFCs with ticagrelor was first assessed by isothermal titration calorimetry assay (Figure 3B). As a control, we also assessed the binding affinity of BSA-PFC nanoparticles with ticagrelor and tirofiban. Each drop into BSA-PFC nanoparticles released only modest heat, especially in the tirofiban group (Figure S7). The calculated Ka values of ticagrelor ($P2Y_{12}$ inhibitor) and tirofiban (GPIIb/IIIa inhibitor) to BSA-PFCs were ~$8.35\times10^4$ $M^{-1}$ and ~$6.76\times10^3$ $M^{-1}$, respectively (Table S3). We next evaluated the binding affinity of PLT-PFC nanoparticles with ticagrelor and
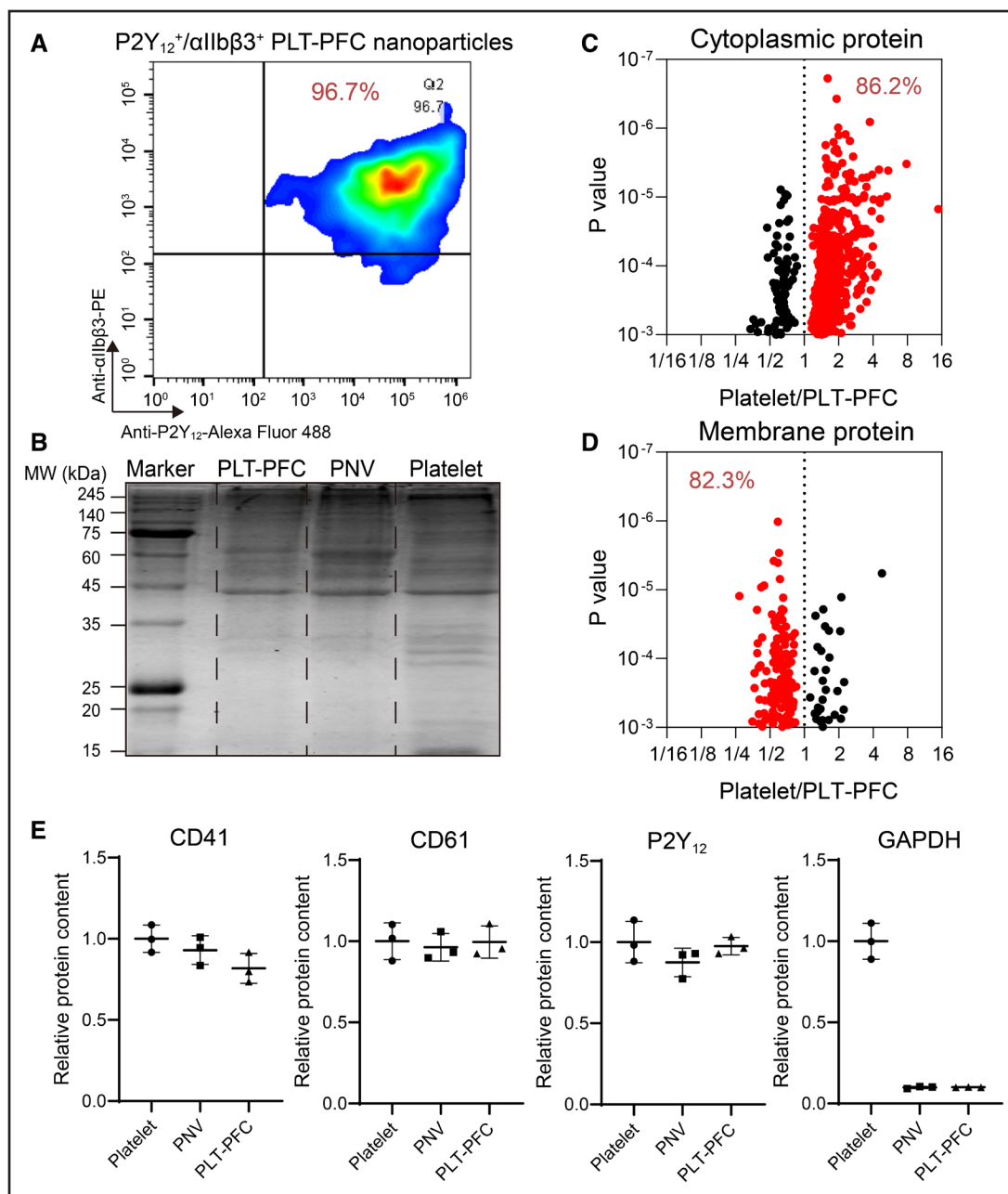
**Figure 2. Functional protein characterization of platelet-mimicking perfluorocarbon-based nanosponges (PLT-PFCs).**
**A**, Nano-flow cytometry validation of key platelet receptors presented on the surface of the PLT-PFC nanoparticles, including αIIbβ3 and P2Y$_{12}$ receptors. **B**, Protein profiles of PLT-PFC, platelet nanovesicles (PNV), and platelet lysates, as analyzed by SDS-PAGE. **C** and **D**, Differential analysis of cytoplasmic (**C**) and membrane (**D**) proteins between platelets and PLT-PFCs (n=3). **E**, Semiquantitative western blot results showed the preservation of membrane surface receptors, CD41, CD61, and P2Y$_{12}$, together with the loss of the platelet intracellular protein marker GAPDH, analyzed by ImageJ software (n=3). GAPDH indicates glyceraldehyde phosphate dehydrogenase.

tirofiban. The Ka value of ticagrelor to PLT-PFC nanoparticles was ~$2.09\times10^5$ M$^{-1}$, which was greater than that of the BSA-PFC nanoparticles in vitro. Moreover, PLT-PFCs showed a greater binding affinity to tirofiban (Ka=$2.31\times10^5$ M$^{-1}$; Figures S8 and S9) than BSA-PFCs. This result corresponds with tirofiban's low plasma protein binding rate of ~65% in whole blood compared with ticagrelor.[25] All these results suggest that PLT-PFCs were likely to exhibit a higher potency in reversing the antiplatelet activity of ticagrelor or tirofiban, which could not be replaced by other nonspecific strategies whose efficacy may become even more compromised in vivo. In addition, the Kd values of PLT-PFCs with ticagrelor or tirofiban, based on the binding curve of PLT-PFCs with ticagrelor (Figure 3C) or tirofiban (Figures S10 and S11) in microscale thermophoresis experiments, were markedly <$1\times10^{-6}$ M (Table S4), further confirming the strong adsorption characteristics of PLT-PFCs for APAs.
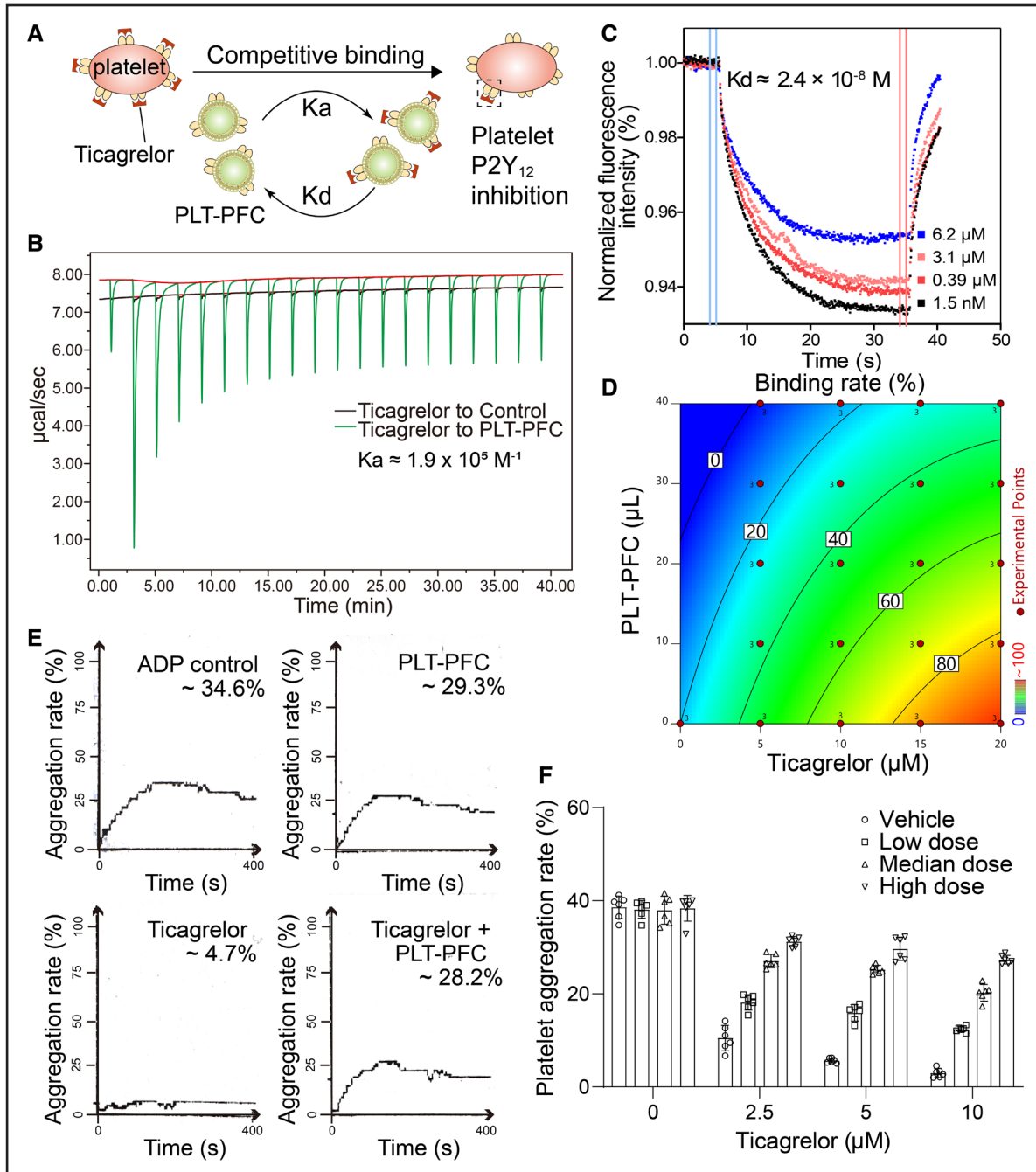
**Figure 3. In vitro binding affinity of platelet-mimicking perfluorocarbon-based nanospones (PLT-PFCs) to antiplatelet agents (APAs) and the reversal of APA activity.**
**A**, Ticagrelor inhibits the platelet P2Y$_{12}$ receptor, which can be competitively reversed by PLT-PFC supplementation. **B**, Isothermal titration calorimetry (ITC) assay of the adsorbing affinity (Ka) of PLT-PFCs for ticagrelor. **C**, Microscale thermophoresis (MST) assay of the dissociation ability (Kd) between PLT-PFCs and ticagrelor. **D**, Fitting analysis of flow cytometry results of ticagrelor inhibiting platelet P2Y$_{12}$ receptors in the presence of a series of PLT-PFCs amounts. Experimental plots applied for the calculations originated from the flow cytometry results. **E**, PLT-PFC supplementation restored platelet aggregation ability, which had been inhibited by ticagrelor. **F**, Human platelet aggregation rate with series concentrations of ticagrelor and PLT-PFC supplementation was quantified. Low, medium, and high dose of PLT-PFCs indicated equivalent doses of 6.7, 13.3, and 26.7×10$^8$ platelet counts/mL, respectively (n=6; $P$-values were assessed by Kruskal-Wallis tests followed by Dunn-Bonferroni post hoc tests. For 4 independent groups comparison in 0 μM of ticagrelor, the overall ANOVA $P$-value=0.89; for 4 independent groups comparison in 2.5 μM of ticagrelor, the overall ANOVA $P$-value = 7.9×10$^{-5}$; for 4 independent groups comparison in 5 μM of ticagrelor, the overall ANOVA $P$-value=7.9×10$^{-5}$; for 4 independent groups comparison in 2.5 μM of ticagrelor, the overall ANOVA $P$-value=7.0×10$^{-5}$.). NS, $P \geq 0.05$, not significant; *$P<0.05$; **$P<0.01$.

The potential transfer of ticagrelor from the PLT-PFCs to uninhibited platelets was due to the reversible binding manner of ticagrelor. However, it does not necessarily affect the overall binding rate of PLT-PFCs to ticagrelor, as the whole transferring process is dynamic and reversible (ie, ticagrelor could also transfer from the temporarily inhibited platelets to PLT-PFCs). This could be better explained by the results on the PLT-PFC dose-dependent reversal of ticagrelor binding onto platelets. Here, a bio-orthogonal chemistry strategy was applied to measure the ticagrelor binding rate. Briefly, the azide group was conjugated with ticagrelor to form ticagrelor-$N_3$ at its terminal hydroxyl group, which does not affect its pharmacological activity.[16,26] Once ticagrelor-$N_3$ bound to platelets in the presence of a series of concentrations of PLT-PFCs, dibenzocyclooctyne-Cy5 was specifically attached to ticagrelor-$N_3$ via a click reaction.[27] The proportion of Cy5-labeled platelets was tested via flow cytometry, and the ticagrelor binding rate was fitted into a suggested quartic fitting model, as shown in Figure 3D and Figure S12. We also conducted platelet aggregation experiments to demonstrate the reversal effect of PLT-PFCs on ticagrelor or tirofiban activity in platelet-rich plasma in vitro. As shown in Figure 3E and Figure S13, ticagrelor and tirofiban both significantly inhibited ADP-induced platelet aggregation. When PLT-PFCs were added to the platelet-rich plasma, ADP-induced platelet aggregation recovered from the ticagrelor or tirofiban inhibition, indicating the successful reversal of APA activity. We also used platelet-rich plasma from healthy human volunteers to verify the efficacy of PLT-PFCs in vitro (Figure 3F). In ticagrelor-spiked samples, PLT-PFCs could effectively correct the ticagrelor-induced inhibition of ADP-triggered platelet aggregation in a dose-dependent manner.[28] On the contrary, PLT-PFC supplementation did not alter the normal platelet aggregation rate as shown in the control group without ticagrelor.

## Pharmacokinetics and Biodistribution of PLT-PFCs

To accurately assess the duration of the reversal effect of PLT-PFC administration, we examined the pharmacokinetics of PLT-PFCs in vivo. Healthy C57BL/6J male mice were intravenously injected with different Cy5.5 fluorescence-labeled drug formulations, including PLT-PFCs, PNVs, or BSA-PFCs. Tail vein blood withdrawn at predetermined time points, within a 24-hour period, was visualized by fluorescence imaging. Both the PLT-PFC and PNV groups exhibited prolonged circulating time in comparison with the BSA-PFC group, indicating that the presence of platelet membranes mitigated the efficient clearance of the nanoparticles from the blood, which was consistent with a previous report.[20] Compared with the PNVs, the PLT-PFCs showed a longer circulating time, suggesting that the more uniform polydispersity

by introduction of the PFC core further improved the pharmacokinetic behavior (Figure 4A). Pharmacokinetic parameters, calculated using a 1-compartment model, indicated that the PLT-PFC group exhibited the longest circulating half-life and the largest area under the curve (AUC; Figure S14). The circulating half-life of PLT-PFC, PNV, or BSA-PFC administration was about ~28, 9, and 2 hours, respectively (Figure S15).

In addition to improving the circulation half-life through surface features, the hydrophilic platelet membrane was used to strengthen the colloidal stability of its nanostructure,[29] as reflected in the markedly smaller polydispersity of PLT-PFCs (Table S2). These properties could prevent the rapid renal excretion upon PLT-PFC collapse, resulting in the prolongation of the circulating time. Morphological differences may also underlie the differential biodistribution between PNVs and PLT-PFCs. Remarkably, the self-assembled PNVs with a larger particle size and polydispersity tended to accumulate in the lung 8 hours post injection, indicating a potential aggregation risk of these PNVs in circulation. Meanwhile, PLT-PFCs, with their more uniform and narrower size distribution, were mainly sequestered by the liver and excreted via the kidney within 24 hours (Figure 4B and 4C).

## In Vivo Blood Elimination and APA Activity Reversal by PLT-PFCs

We next evaluated the plasma pharmacokinetic profiles of ticagrelor or tirofiban with the treatment of saline, PLT-PFC (equivalent dose of $1\times10^9$ platelet counts/kg), high-dose platelet ($1\times10^9$ counts/kg), or standard-dose platelet ($2\times10^8$ counts/kg) injections, respectively (the equivalent dose of $1\times10^9$ platelet counts/kg means that the injected dose of PLT-PFCs was prepared from $1\times10^9$ platelets/kg of mouse weight). We calculated the standard dose from the recommended dose in clinical guidelines on platelet transfusion.[10] After a 20 mg/kg ticagrelor intravenous injection, the plasma concentration of free ticagrelor in the absence of PLT-PFC (or platelet) transfusion reached a plateau of 8.8±2.1 µM within 10 minutes (Figure 5A). The plasma concentration of ticagrelor then gradually decreased to ~1 µM at 8 hours post injection. Ticagrelor showed an estimated half-life of ~13.4±1.1 hours and an estimated AUC of 144.5±31.0 µM·hours in C57BL/6 male mice (Figure 5B). To investigate ticagrelor activity reversal, the standard or high doses of platelets, or PLT-PFC transfusion, were administered when the plasma ticagrelor concentration reached its highest level. At subsequent time points, both high-dose platelet and PLT-PFC transfusion effectively decreased the ticagrelor concentration (Table S7). The half-life of ticagrelor in the high-dose platelet transfusion group was 14.7±1.9 hours and the AUC was 35.1±12.2 µM·hours. Meanwhile, the half-life of ticagrelor in the PLT-PFC treated group was 13.4±1.1 hours
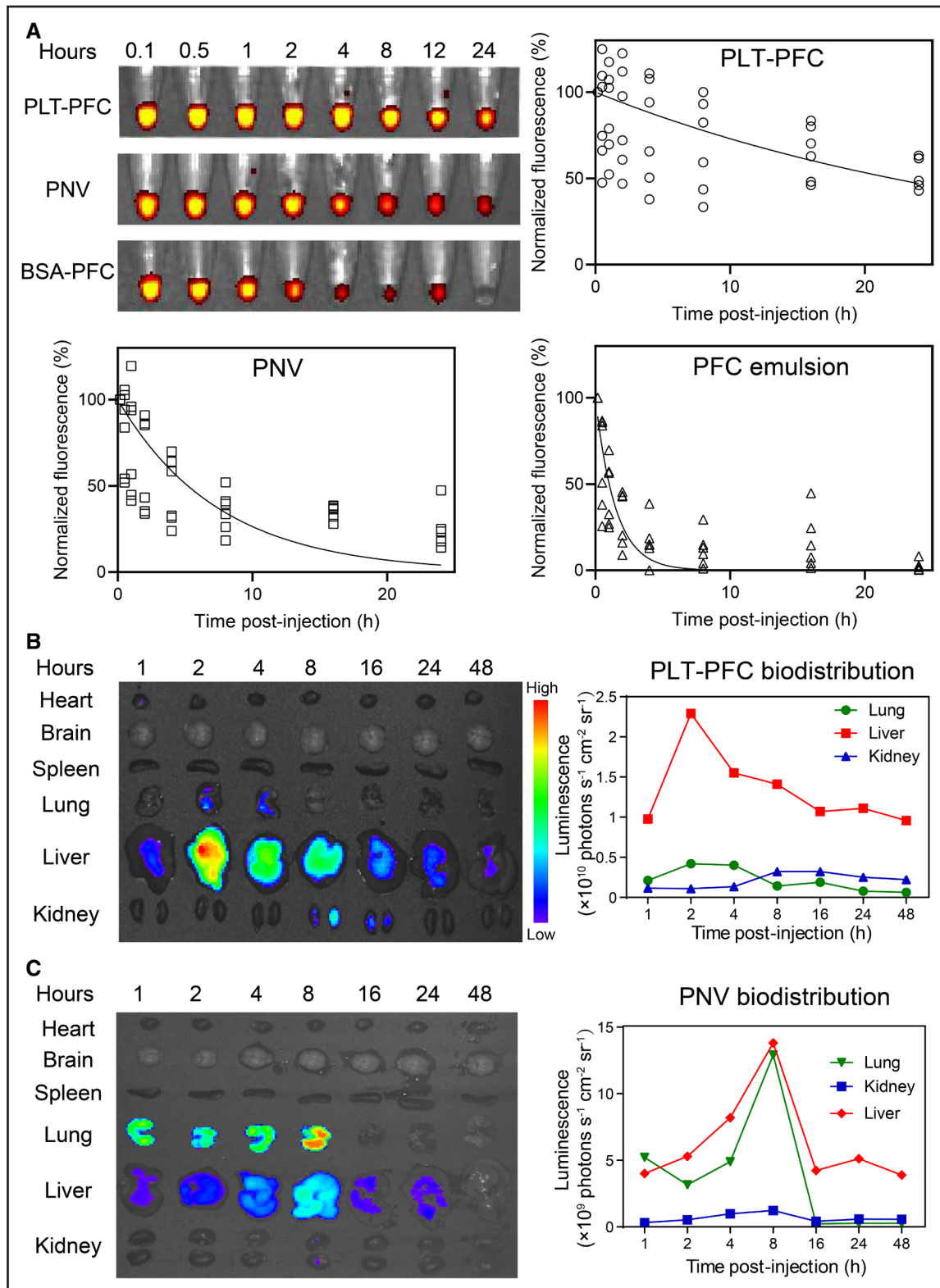
**Figure 4. Blood pharmacokinetics and biodistribution of platelet-mimicking perfluorocarbon-based nanosponges (PLT-PFCs).**
**A**, Representative fluorescence images (**left**) and quantification (**right**) of blood samples derived from mice treated with Cy5.5-labeled PLT-PFCs, platelet nanovesicles (PVNs), or BSA-PFCs administered at predetermined time points (n=6). **B** and **C**, Representative images (**left**) and quantification (**right**) of the biodistribution of PLT-PFC (**B**) and PNV (**C**) nanoparticles in the major organs, including heart, brain, spleen, lung, liver, and kidney, at the indicated time points. Quantitative results were presented in Figure S27.
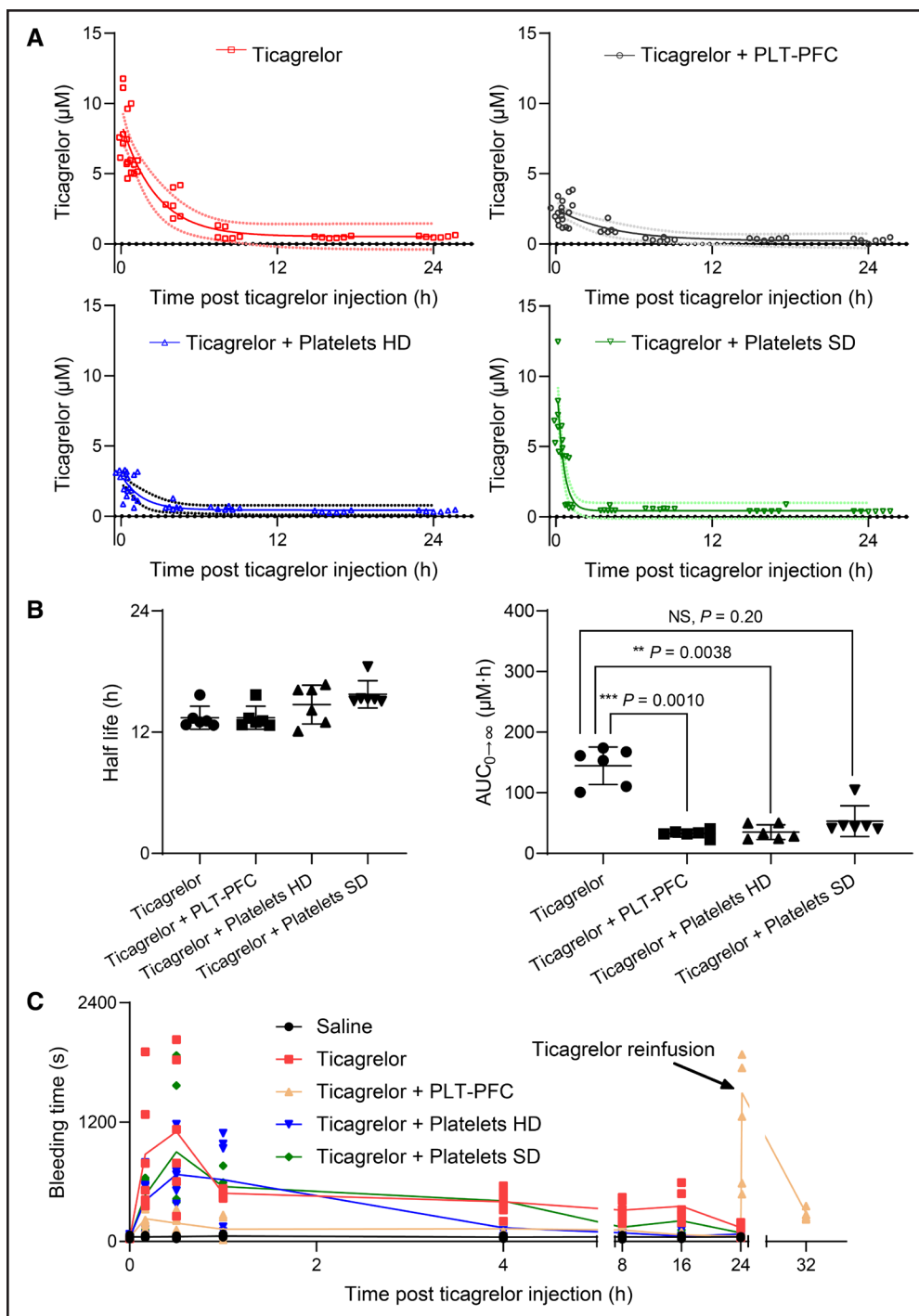
**Figure 5. In vivo blood elimination and reversal of ticagrelor activity by platelet-mimicking perfluorocarbon-based nanosponges (PLT-PFCs).**

**A**, High performance liquid chromatography (HPLC) quantification of ticagrelor in plasma derived from mice treated with ticagrelor, ticagrelor+PLT-PFC transfusion, ticagrelor + high-dose platelet transfusion, or ticagrelor+standard-dose platelet transfusion at predetermined time points post ticagrelor injection. **B**, The pharmacokinetic behavior of ticagrelor was analyzed, including its half-life and area under the curve (AUC), calculated using a linear 1-compartment model. High dose (HD), $1\times10^9$ platelet counts/kg; standard dose (SD), $2\times10^8$ platelet counts/kg (n=6; $P$-values were assessed by Kruskal-Wallis tests [multiple groups] followed by Dunn-Bonferroni post hoc tests. For 4 independent groups comparison in the **left**, the overall ANOVA $P$-value=0.12; for 4 independent groups comparison in the **right**, the overall ANOVA $P$-value=0.0012.). **C**, Tail bleeding time of mice treated with saline, ticagrelor, ticagrelor+PLT-PFC transfusion, ticagrelor+high-dose platelet transfusion, or ticagrelor+standard-dose platelet transfusion at the indicated time points. The antiplatelet effect was immediately realized upon ticagrelor reinfusion. (n=6); NS, $P\geq0.05$, not significant; *$P<0.05$; **$P<0.01$.

and the AUC was 32.8±5.9 μM·hours. However, platelet transfusion at the standard dose induced an inadequate decrease in plasma ticagrelor, as manifested by the similar AUC (53.1±25.3 μM·hours). This dose-dependent ticagrelor elimination from blood by platelet transfusion corresponds to previous reports,[11] indicating the limited ability of platelet transfusion to reverse the activity of platelet inhibitors due to the limited transfusion dose.

In parallel, we also investigated the plasma pharmacokinetic profiles of tirofiban under the same conditions we used for ticagrelor. PLT-PFC or platelet transfusion elicited a similar reversal trend in the pharmacokinetic behavior of tirofiban as that of ticagrelor (Figure S16 and Table S8). Interestingly, in both the tirofiban- and ticagrelor-treated groups, the changes in the overall AUC were more statistically significant than changes in the half-lives (Figure 5B; Figure S16B). One possible explanation for the inconsistent significance between AUC and half-life was that the PLT-PFCs, with its longer circulation time (half-life=~1 day; Figure S15), acted as a ticagrelor (or tirofiban)-specific nanosponge in the plasma and, through sequestration, had less effect on accelerating the excretion of the APAs (Figure 4A and 4B; Figures S14 and S15). This feature of PLT-PFCs made it possible to use a single injection, avoiding a prolonged intravenous drip.

We next recorded the tail bleeding time of mice treated with the different regimens at predetermined time points (Figure 5C). Compared with saline-treated mice, the bleeding time of tirofiban- or ticagrelor-treated mice rapidly increased post injection for 0.5 hours and gradually returned to the normal level within 24 hours. Both high-dose platelet transfusion and standard-dose platelet transfusion had negligible effects on the increased bleeding time posttreatment with ticagrelor. In contrast, PLT-PFC treatment significantly reversed the elevated bleeding time, more rapidly returning it to normal levels seen in the control group (Table S9). Upon re-injection of ticagrelor or tirofiban after 24 hours in the PLT-PFC treated group, the bleeding time increased within 0.5 hours, indicating the APAs could function again in the PLT-PFC treated mice after 1 day, which was desirable in clinical practice. When PLT-PFCs were administered at a lower dose (equivalent dose of $2\times10^8$ platelet counts/kg) compared to the effective dose described above (equivalent dose of $1\times10^9$ platelet counts/kg), the reversal effect against ticagrelor was compromised accordingly, but still effective compared to the no treatment group. Conversely, a high dose of PLT-PFCs (equivalent dose of $5\times10^9$ platelet counts/kg) did not contribute to a more significant change in bleeding time. Taken together, the dose-response relationship showed a positive correlation between the dose of PLT-PFC administration and the corresponding pharmacological activity under therapeutic dosage (Figure S17). These results demonstrate that PLT-PFC injection can effectively reverse

APA activity in vivo without eliciting a rebound in platelet activity.

To explore the potency of PLT-PFC in reversing irreversible antiplatelet drugs, we investigated the bleeding time in aspirin-administered mice with or without PLT-PFC treatment. Interestingly, the bleeding time showed no statistical difference in the presence of PLT-PFCs. This result indicated that the reversal effect of PLT-PFCs may not be useful to reverse the irreversible antiplatelet drug aspirin. On the contrary, this result also ruled out the potential off-target pro-hemostatic effect of PLT-PFC treatment that may otherwise interfere the bleeding time test in ticagrelor and tirofiban reversal studies (Figure S18).

## In Vivo Functional Reversal of APAs in a Hemorrhagic Transformation Mouse Model

Long-term antiplatelet therapy has been shown to increase the perioperative risk of intracranial hemorrhage after thrombolytic therapy in ischemic stroke patients.[30,31] Therefore, an immediate cease of APA usage before thrombolysis was suggested.[32,33] With this scenario in mind, we investigated whether PLT-PFC treatment had the potential to mitigate the bleeding risk of thrombolytic therapy in an experimental stroke model in which the animals were pretreated with undesirable antiplatelet therapy. The experimental timeline was presented in Figure 6A. Magnetic resonance imaging was applied to each model mouse to simultaneously observe any hemorrhage and thrombosis in susceptibility weighted imaging and T2-weighted imaging mode, respectively (Figure 6B). According to the magnetic resonance imaging results, PLT-PFC treatment before thrombolysis significantly decreased the hemorrhagic area (Figure S19). Meanwhile, the thrombotic area did not expand within a week after the treatment (Figure S20). The hemorrhage site correlated with the infarction site, and few hemorrhagic spots were observed in the contralateral hemisphere (Figures S19 through S21). The hemorrhagic area was also visualized by Evans blue staining and fluorescence imaging. Consistent with a previous study as well as our magnetic resonance imaging results, both tirofiban and ticagrelor treatment exacerbated hemorrhage after thrombolytic therapy in the stroke model.[32] Tirofiban (5 mg/kg) elicited a relatively more severe bleeding risk compared with ticagrelor (20 mg/kg; Figure 6C and 6D). The fluorescence intensity ratio of the right brain to the left brain in the PLT-PFC-treated group was much smaller than that in the saline group, indicating a decreased hemorrhagic risk due to PLT-PFC treatment. Furthermore, we used triphenyl tetrazolium chloride staining to identify the infarct area in the different treatment groups (Figure 6E). Similar infarct areas were observed among all groups, indicating that the progression of lesion size was not (at least not directly) responsible for the hemorrhagic transformation.
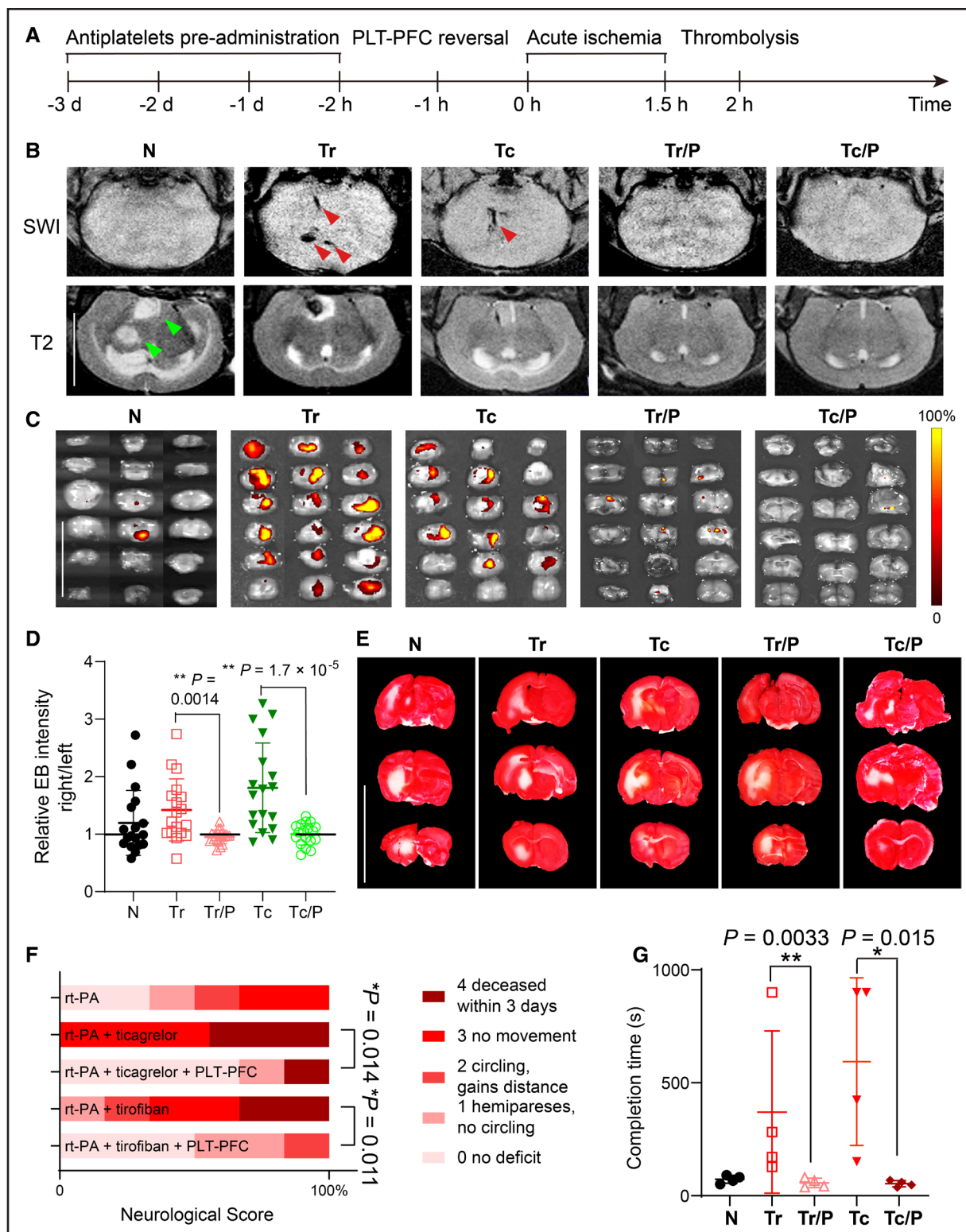
**Figure 6. In vivo reversal of antiplatelet agent (APA) activity in the hemorrhagic transformation mouse model.**
**A**, Experimental timeline for the administration of various drug formulations in the middle cerebral artery occlusion (MCAO) mouse model pretreated with APA and rt-PA. **B**, Magnetic resonance imaging of hemorrhage and thrombosis in brains from platelet-mimicking perfluorocarbonbased nanosponge (PLT-PFC)-treated mice (n=6 for N group; n=4 for Tr group; n=5 for Tc group; n=6 for Tr/P group; n=5 for Tc/P group, respectively, as shown in Figures S13 and S14; Scale bar = 5 mm). Susceptibility weighted imaging (SWI) was applied to identify the hemorrhagic spots (red arrows); T2-weighted imaging was applied to identify infarctions (green arrows). **C**, Evans blue (EB) extravasation in brains from PLT-PFC-treated mice (n=3; Scale bar = 2 cm). **D**, Bilateral comparison of EB extravasation in brains from PLT-PFC-treated mice (n=18). *P*-values between 2 groups were assessed by Kruskal-Wallis test followed by Dunn-Bonferroni post hoc tests. For multiple-group comparison, the overall ANOVA *P*-value=3.8×10⁻⁵. **E**, Triphenyl tetrazolium chloride (TTC) staining of (*Continued*)

All these results suggested that long-term administration of antiplatelet therapy at high dosage before thrombolysis therapy significantly increased bleeding risk while offering limited improvement in the ischemic stroke model. Significantly, PLT-PFC pretreatment effectively eliminated the bleeding risk caused by antiplatelet therapy, enabling urgent vascular recanalization without delay due to inadequate APA usage. To evaluate the benefits gained by PLT-PFC treatment on behavior, we attained neurological scores for the mice in the different treatment groups. The improved neurological scores and movement frequency in the PLT-PFC group again revealed functional reversal in the activity of APAs before thrombolytic therapy in the mice model (Figure 6F and 6G).

## Loss of Thrombogenic Potential of PLT-PFCs Due to its Inert Core Compared to Living Platelets

Although platelet transfusion shows the potential to reverse the antiplatelet effects of $P2Y_{12}$ inhibitors in a dose-dependent manner similar to PLT-PFC transfusion, overdose platelet transfusion often carries serious thrombotic risks, including thrombosis events induced by thrombogenic substances, such as plasminogen activator inhibitors, platelet-activating factors, and thrombospondin, released from activated platelets.[12,15,17,34] In our work, the thrombotic triggers within platelets were removed during the preparation of the PLT-PFC nanoparticles; therefore, PLT-PFCs were no longer activable (Figure 7A).[35] To investigate the difference in aggregation behavior between normal platelets and PLT-PFCs, FITC-labeled fibrinogen was precoated onto glass slides, followed by incubation of the slides with Rho6G-labeled platelets, PLT-PFCs, or BSA-PFCs suspended in ADP containing modified Tyrode's buffer. As shown in Figure 7B, confocal microscopy revealed clustered aggregates in the Rho6G-labeled platelet group. In comparison, almost no fluorescence-labeled BSA-PFCs were observed due to the absence of any fibrinogen-binding receptors. Excessive platelet activation causes clot retraction, which further consolidates the integrity of blood clots by squeezing circulating blood cells.[36] Therefore, we next examined whether PLT-PFCs could induce the clot retraction process, which is directly driven by the intrinsic thrombotic activity in live platelets. Red blood cells were added to track the blood clot supported by the fibrin network. As shown in Figure 7C, platelet-rich plasma elicited a major conformational change in the shape of the blood clots. In contrast, platelet poor plasma did not retract the fibrin network, even in the presence of PLT-PFCs, indicating a potential lack of thrombogenic outside-in signaling. In addition, after treatment with PLT-PFCs, there was no statistically significant change in the major blood coagulation parameters, including activated partial thromboplastin time, prothrombin time, fibrinogen concentration, and thrombin time. Compared with other groups, high-dose platelet transfusion led to a significantly elevated hypercoagulable state (Figure 7D through 7G). Correspondingly, platelet transfusion also increased the platelet number (platelet counts, Figure S22A) and plateletcrit (Figure S22D), while the mean platelet volume (Figure S22B) and platelet distribution width (Figure S22C) did not show statistical difference. In contrast, PLT-PFC administration did not show any effect on platelet count and plateletcrit in vivo. We further examined the possible immunogenicity of PLT-PFC administration by ELISA. As shown in Figure S23, no apparent statistical difference was detected in the levels of serum TNF (tumor necrosis factor)-$\alpha$ and IFN (interferon)-$\gamma$ in mice treated with PLT-PFCs within 7 days post injection. Collectively, safety tests of PLT-PFCs were carried out in mice where no or few side effects were observed, including inflammatory responses (Figure S23), neutropenia (Figure S24), thrombocytopenia (Figure S22), hypotension/tachycardia responses (Figure S25), flu-like symptoms, or any histological changes in major organs (Figure S26) under therapeutic dosage of PLT-PFCs, as reported in previous studies on PFC-based nanoparticles.[37]

## DISCUSSION

In the present study, we developed an antiplatelet reversal agent by coating platelet membrane onto the surface of PFC cores to form PLT-PFCs. The key platelet surface receptors are retained on PLT-PFCs, which can selectively bind the APAs to achieve effective functional reversal. Unlike platelet transfusion, the absence of intrinsic thrombotic activity in the PLT-PFCs did not introduce thrombotic risk. PLT-PFCs also significantly ameliorated the severity of hemorrhagic transformation in ischemic mice treated with antiplatelet and thrombolytic agents, improving neurological scores without bringing additional thrombotic risk. Taken together, our results demonstrate that PLT-PFCs possess both high binding affinity with APAs in vitro and functional reversal of APAs in vivo.

---

**Figure 6 Continued.** brains from mice treated with the indicated drug formulations to identify the infarct area (n=3; Scale bar = 1 cm). **F**, Neurological scores in the different groups of mice (in percentage of mice per group; n=6 for rt-PA, rt-PA+ticagrelor+PLT-PFC, rt-PA+tirofiban, rt-PA+tirofiban+PLT-PFC group; n=9 for rt-PA+ticagrelor group). *P*-value among all groups was assessed by Kruskal-Wallis test; *P*-values between 2 groups were assessed by Mann-Whitney *U* tests. For multiple-group comparison, the overall ANOVA *P*-value=0.0019. **G**, Completion time of cylinder test in the different groups (n=4). *P*-value among all groups was assessed by Kruskal-Wallis test; *P*-values between 2 groups were assessed by Dunn's post hoc tests. For multiple-group comparison, the overall ANOVA *P*-value=0.0049. In (**B**) through (**E**) and (**G**), the group numbers indicate the following: N, MCAO model; Tr, tirofiban-treated group; Tc, ticagrelor-treated group; Tr/P, tirofiban+PLT-PFC-treated group; Tc/P, ticagrelor+PLT-PFC-treated group. *$P$<0.05; **$P$<0.01.
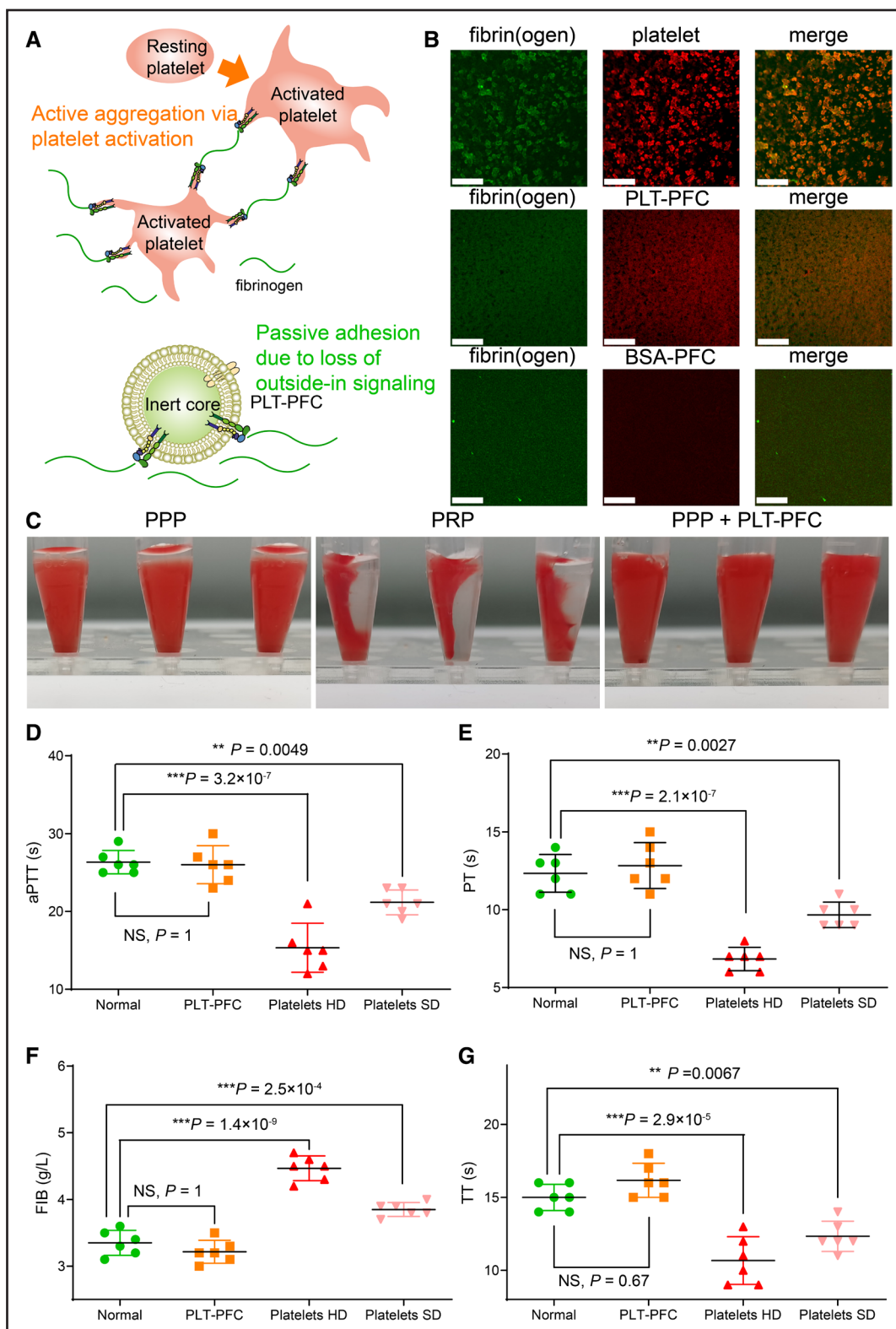
**Figure 7. Loss of thrombogenic potential of platelet-mimicking perfluorocarbon-based nanosponges (PLT-PFCs) due to the inactive core compared to living platelets.**

**A**, Schematic illustration of the differential aggregation behavior of platelets and PLT-PFCs. Upon attachment to the damaged endothelium, platelets are activated and can further secrete thrombogenic substances to activate more resting platelets. PLT-PFCs cannot secrete thrombogenic substances to activate more platelets due to the inactive core. **B**, Fibrinogen adhesion test of platelets, PLT-PFCs, and BSA-PFCs. Scale bar = 40 μm. **C**, Representative images of blood samples subjected to the clot retraction assay with platelet poor plasma (PPP), platelet-rich plasma (PRP), and PRP+PLT-PFCs. **D** through **G**, Coagulation indicators of plasma from mice (activated partial thromboplastin time [aPTT], fibrinogen concentration[FIB], prothrombin time [PT] and thrombin time [TT]) post injection with the indicated (*Continued*)

In the current work, we observed that PLT-PFCs could bind to collagen, fibrinogen, and von Willebrand factor partially by their corresponding receptors. The specific binding process is similar to platelet adhesion, which is indispensable for the physiological platelet activation process. Therefore, a prohemostatic hypothesis of action brought on by PLT-PFC incorporation into a forming hemostatic plug or thrombus may seem reasonable. Recent studies have focused on synthetic nanoparticles decorated with motifs such as specific peptides that can selectively bind to collagen,[38] GPIIb-IIIa,[39] or von Willebrand factor,[40] to achieve hemostatically relevant outputs. While these strategies based on platelet adhesion mechanisms could serve as potent hemostats, the overall hemostatic effect was still limited in vivo compared to platelets.[41] Instead, the synthetic platelet technologies (ie, SynthoPlate) are making exciting advances. The heteromultivalent modification strategy taking advantage of more combinatorial platelet activation processes (including adhesion, aggregation, thrombin amplification, secretion, and clot retraction) has become a critical principle in hemostats development, especially the phosphatidylserine exposure process.[42] PLT-PFC only retained platelet surface proteins with limited phosphatidylserine exposure, thus the prohemostatic effect was negligible. On the contrary, PLT-PFC may act as a sink for ligands including adenosine diphosphate and fibrinogen especially in antiplatelet drug-free blood, which may counteract its prohemostatic potential. Compared to the mechanisms of action of other platelet-inspired hemostatic technologies, such as the synthetic platelets and thrombosomes,[43] PLT-PFCs were designed to focus on functional reversal of APAs in specialized clinical scenarios where the therapeutic effects of alternative vascular recanalization strategies should not be compromised. Existing platelet-inspired technologies mainly focus on reducing contamination risks and increasing platelet shelf-life in vivo and storage in vitro.[42]

PFC is a type of fluorine-abundant material often employed to create low-adhesive surfaces in vivo, due to its inertness and biocompatibility within blood vessels.[44] PFC has most commonly been utilized as a surface coating material in coronary drug eluting stents to prevent stent thrombogenicity.[45] In our study, the utilization of PFC as the inactive core effectively enhanced the stability of membrane-based nanoparticles, affording them a prolonged circulating time in comparison with PNV without PFC core. Although we demonstrated effective functional reversal of APAs in human blood, additional preclinical studies are still required, for example, optimization of the pharmacokinetic or pharmacodynamic behavior of PLT-PFCs and a fine tuning of the ratio of platelet membranes and PFC according to the variable pharmacokinetics of different APAs. Moreover, PFC has been shown to serve as an oxygen-carrying material.[20] Thus, PLT-PFCs may be used for targeted delivery of oxygen to ischemic tissue to alleviate necrosis in myocardial infarction or stroke. The efficacy of PLT-PFCs against irreversible inhibitors (eg, clopidogrel), cytoplasmic inhibitors (eg, aspirin), and their relative active metabolites also needs to be explored.

The major challenge of clinical usage of PLT-PFCs may be the difficulty in its purification process. In clinical platelet transfusion, if few leukocytes contaminate the platelet products, the recipients may acquire alloimmunization reactions to cause rapid removal of transfused platelets, especially in the repeatedly transfused patients, which is termed as platelet refractoriness.[10] The incidence rate of platelet refractoriness can be minimized by purifying platelet products, such as filter leukoreduction, UV-B irradiation, or pathogen inactivation.[46] A further approach to eradicate this problem may be the development of mass production techniques from precursor cells (eg, megakaryocytes) or induced pluripotent stem cells.[47,48] Another concern for the purification process may be the flipping of phosphatidylserine to the outer surface of the isolated membrane, which raises the potential of coagulation. Although the PS-positive percentage of PLT-PFCs was limited, as shown above (Figure S6), we still consider the retention of PS on the surface of the nanomedicine as a major concern in regard to future clinical translation. In this design, we mainly used the combined methods of freeze–thawing and coextrusion. Although platelet membrane-cloaked nanoparticles have been proven to show a right-side-out membrane orientation,[49] additional efforts may be still required to discover the exact dynamic change of platelets during these unnaturally occurring processes. Future studies may focus on the potential biosafety profiles of the retained platelet cytoplasmic proteins on PLT-PFCs. To date, we have not observed any obvious side effects on PLT-PFC-treated mice under the current therapeutic dosage. In terms of storage, platelet products cannot be lyophilized. This is because platelets are living cells that are sensitive to the culturing and storing conditions. However, the functional motifs of PLT-PFCs are their platelet receptors with proper conformation. Therefore, the PLT-PFC nano-formulation can be lyophilized and has been proven to maintain its pharmacological activity after 6 months of storage (Figure S1).

Despite those challenges for PLT-PFC mass production, we still consider that the demand for antiplatelet

**Figure 7 Continued.** drug formulations (n=6; all groups passed Shapiro-Wilks normality tests [$\alpha$=0.05]. For comparisons among multiple groups, 1-way ANOVA tests followed by Bonferroni post hoc tests were carried out.). **D**, For multiple-group comparison, the overall ANOVA P-value=$1.1\times10^{-7}$. **E**, For multiple-group comparison, the overall ANOVA P-value=$2.0\times10^{-8}$. **F**, For multiple-group comparison, the overall ANOVA P-value=$8.8\times10^{-11}$. **G**, For multiple-group comparison, the overall ANOVA P-value=$5.0\times10^{-7}$.

reversal treatment outweighs the manufacturing difficulties and cost. Hopefully, further comprehensive insights into the role of platelets will facilitate the development of platelet-inspired nanomedicine applied in more clinical scenarios.[42] Overall, our strategy holds great promise for prophylactically and therapeutically improving the clinical benefits of antiplatelet therapy.

## REFERENCES

1. Vos T, Lim SS, Abbafati C, Abbas KM, Abbasi M, Abbasifard M, Abbasi-Kangevari M, Abbastabar H, Abd-Allah F, Abdelalim A, et al. Global burden of 369 diseases and injuries in 204 countries and territories, 1990–2019: a systematic analysis for the Global Burden of Disease Study 2019. *The Lancet*. 2020;396:1204–1222. doi: https://doi.org/10.1016/S0140-6736(20)30925-9

2. Mackman N, Bergmeier W, Stouffer GA, Weitz JI. Therapeutic strategies for thrombosis: new targets and approaches. *Nat Rev Drug Discov*. 2020;19:333–352. doi: 10.1038/s41573-020-0061-0

3. Xu J, Zhang Y, Nie G. Intelligent antithrombotic nanomedicines: Progress, opportunities, and challenges. *VIEW*. 2021;2:20200145. doi: 10.1002/viw.20200145

4. McFadyen JD, Schaff M, Peter K. Current and future antiplatelet therapies: emphasis on preserving haemostasis (vol 15, pg 181, 2018). *Nat Rev Cardiol*. 2018;15:181192–181191. doi: 10.1038/nrcardio.2017.206

5. Joyce LC, Baber U, Claessen BE, Sartori S, Chandrasekhar J, Cohen DJ, Henry TD, Ariti C, Dangas G, Faggioni M, et al. Dual-Antiplatelet therapy cessation and cardiovascular risk in relation to age analysis from the PARIS registry. *Jacc-Cardiovasc Inte*. 2019;12:983–992. doi: 10.1016/j.jcin.2019.02.033

6. Plow EF, Wang YM, Simon DI. The search for new antithrombotic mechanisms and therapies that may spare hemostasis. *Blood*. 2018;131:1899–1902. doi: 10.1182/blood-2017-10-784074

7. Keaney JF Jr. Balancing the risks and benefits of dual platelet inhibition. *N Engl J Med*. 2015;372:1854–1856. doi: 10.1056/nejme1502137

8. Wallentin L, Becker RC, Budaj A, Cannon CP, Emanuelsson H, Held C, Horrow J, Husted S, James S, Katus H, et al. Ticagrelor versus clopidogrel in patients with acute coronary syndromes. *N Engl J Med*. 2009;361:1045–1057. doi: 10.1056/nejmoa0904327

9. Bonaca MP, Bhatt DL, Cohen M, Steg PG, Storey RF, Jensen EC, Magnani G, Bansilal S, Fish MP, Im K, et al. Long-term use of ticagrelor in patients with prior myocardial infarction. *New Engl J Med*. 2015;372:1791–1800. doi: 10.1056/Nejmoa1500857

10. Estcourt LJ, Birchall J, Allard S, Bassey SJ, Hersey P, Kerr JP, Mumford AD, Stanworth SJ, Tinegate H, Haematology BCS. Guidelines for the use of platelet transfusions. *Br J Haematol*. 2017;176:365–394. doi: 10.1111/bjh.14423

11. Godier A, Taylor G, Gaussem P. Inefficacy of platelet transfusion to reverse ticagrelor. *N Engl J Med*. 2015;372:196–197. doi: 10.1056/nejmc1409373

12. Baharoglu MI, Cordonnier C, Salman RA-S, de Gans K, Koopman MM, Brand A, Majoie CB, Beenen LF, Marquering HA, Vermeulen M, et al. Platelet transfusion versus standard care after acute stroke due to spontaneous cerebral haemorrhage associated with antiplatelet therapy (PATCH): a randomised, open-label, phase 3 trial. *The Lancet*. 2016;387:2605–2613. doi: 10.1016/s0140-6736(16)30392-0

13. O'Connor SA, Amour J, Mercadier A, Martin R, Kerneis M, Abtan J, Brugier D, Silvain J, Barthelemy O, Leprince P, et al. Efficacy of ex vivo autologous and in vivo platelet transfusion in the reversal of P2Y(12) inhibition by clopidogrel, prasugrel, and ticagrelor the APTITUDE study. *Circ-Cardiovasc Inte*. 2015;8:e002786. doi: 10.1161/CIRCINTERVENTIONS.115.002786

14. Trenk D, Hille L, Leggewie S, Stratz C, Nuhrenberg TG, Aradi D, Schror K, Sibbing D. Antagonizing P2Y12 receptor inhibitors: current and future options. *Thromb Haemost*. 2019;119:1606–1616. doi: 10.1055/s-0039-1693738

15. Frontera JA, Lewin JJ 3rd, Rabinstein AA, Aisiku IP, Alexandrov AW, Cook AM, del Zoppo GJ, Kumar MA, Peerschke EI, Stiefel MF, et al. Guideline for reversal of antithrombotics in intracranial hemorrhage: a statement for healthcare professionals from the neurocritical care society and society of critical care medicine. *Neurocritical care*. 2016;24:6–46. doi: 10.1007/s12028-015-0222-x

16. Buchanan A, Newton P, Pehrsson S, Inghardt T, Antonsson T, Svensson P, Sjogren T, Oster L, Janefeldt A, Sandinge AS, et al. Structural and functional characterization of a specific antidote for ticagrelor. *Blood*. 2015;125:3484–3490. doi: 10.1182/blood-2015-01-622928

17. Xu JC, Zhang YL, Xu JQ, Liu GN, Di CZ, Zhao X, Li X, Li Y, Pang NB, Yang CZ, et al. Engineered nanoplatelets for targeted delivery of plasminogen activators to reverse thrombus in multiple mouse thrombosis models. *Adv Materials*. 2020;32:1905145. doi: 10.1002/Adma.201905145

18. Wei XL, Ying M, Dehaini D, Su YY, Kroll AV, Zhou JR, Gao WW, Fang RH, Chien S, Zhang LF. Nanoparticle functionalization with platelet membrane enables multifactored biological targeting and detection of atherosclerosis. *ACS Nano*. 2018;12:109–116. doi: 10.1021/acsnano.7b07720

19. Liu GN, Zhao X, Zhang YL, Xu JC, Xu JQ, Li Y, Min H, Shi J, Zhao Y, Wei JY, et al. Engineering biomimetic platesomes for pH-responsive drug delivery and enhanced antitumor activity. *Adv Materials*. 2019;31:1900795. doi: 10.1002/Adma.201900795

20. Zhuang J, Ying M, Spiekermann K, Holay M, Zhang Y, Chen F, Gong H, Lee JH, Gao W, Fang RH, et al. Biomimetic nanoemulsions for oxygen delivery in vivo. *Adv Mater*. 2018;30:1804693. doi: 10.1002/adma.201804693

21. Gao M, Liang C, Song XJ, Chen Q, Jin QT, Wang C, Liu Z. Erythrocyte-membrane-enveloped perfluorocarbon as nanoscale artificial red blood cells to relieve tumor hypoxia and enhance cancer radiotherapy. *Adv Materials*. 2017;29:1701429. doi: 10.1002/Adma.201701429

22. Hoshyar N, Gray S, Han HB, Bao G. The effect of nanoparticle size on in vivo pharmacokinetics and cellular interaction. *Nanomedicine-Uk*. 2016;11:673–692. doi: 10.2217/nnm.16.5

23. Boada C, Zinger A, Tsao C, Zhao P, Martinez JO, Hartman K, Naoi T, Sukhoveshin R, Sushnitha M, Molinaro R, et al. Rapamycin-loaded biomimetic nanoparticles reverse vascular inflammation. *Circ Res*. 2020;126:25–37. doi: 10.1161/CIRCRESAHA.119.315185

24. Baig AA, Haining EJ, Geuss E, Beck S, Swieringa F, Wanitchakool P, Schuhmann MK, Stegner D, Kunzelmann K, Kleinschnitz C, et al. TMEM16F-mediated platelet membrane phospholipid scrambling is critical for hemostasis and thrombosis but not thromboinflammation in mice-brief report. *Arterioscler Thromb Vasc Biol*. 2016;36:2152–2157. doi: 10.1161/atvbaha.116.307727

25. Kondo K, Umemura K. Clinical pharmacokinetics of tirofiban, a nonpeptide glycoprotein IIb/IIIa receptor antagonist - Comparison with the monoclonal antibody abciximab. *Clin Pharmacokinet*. 2002;41:187–195. doi: 10.2165/00003088-200241030-00003

26. Geranpayehvaghei M, Shi QW, Zhao BC, Li SP, Xu JC, Taleb M, Qin H, Zhang YL, Khajeh K, Nie GJ. Targeting delivery of platelets inhibitor to prevent tumor metastasis. *Bioconjug Chem.* 2019;30:2349–2357. doi: 10.1021/acs.bioconjchem.9b00457

27. Qin H, Zhao R, Qin Y, Zhu J, Chen L, Di C, Han X, Cheng K, Zhang Y, Zhao Y, et al. Development of a cancer vaccine using in vivo click-chemistry-mediated active lymph node accumulation for improved immunotherapy. *Adv Mater.* 2021;33:e2006007. doi: 10.1002/adma.202006007

28. Bhatt DL, Pollack CV, Weitz JI. Antibody-based ticagrelor reversal agent in healthy volunteers reply. *New Engl J Med.* 2019;381:586–586. doi: 10.1056/NEJMoa1901778

29. Luk BT, Hu CM, Fang RH, Dehaini D, Carpenter C, Gao W, Zhang L. Interfacial interactions between natural RBC membranes and synthetic polymeric nanoparticles. *Nanoscale.* 2014;6:2730–2737. doi: 10.1039/c3nr06371b

30. Altersberger VL, Sturzenegger R, Raty S, Hametner C, Scheitz JF, Moulin S, van den Berg SA, Zini A, Nannoni S, Heldner MR, et al. Prior dual antiplatelet therapy and thrombolysis in acute stroke. *Ann Neurol.* 2020;88:857–859. doi: 10.1002/ana.25850

31. Ye Y, Zhang FT, Wang XY, Tong HX, Zhu YT. Antithrombotic agents for tPA-induced cerebral hemorrhage: a systematic review and meta-analysis of preclinical studies. *Journal of the American Heart Association.* 2020;9:e017876. doi: 10.1161/JAHA.120.017876

32. Zheng Y, Lieschke F, Schaefer JH, Wang X, Foerch C, van Leyen K. Dual antiplatelet therapy increases hemorrhagic transformation following thrombolytic treatment in experimental stroke. *Stroke.* 2019;50:3650–3653. doi: 10.1161/strokeaha.119.027359

33. Robinson TG, Wang X, Arima H, Bath PM, Billot L, Broderick JP, Demchuk AM, Donnan GA, Kim JS, Lavados PM, et al. Low-versus standard-dose alteplase in patients on prior antiplatelet therapy the ENCHANTED trial (Enhanced Control of Hypertension and Thrombolysis Stroke Study). *Stroke.* 2017;48:1877–1883. doi: 10.1161/strokeaha.116.016274

34. Swan D, Loughran N, Makris M, Thachil J. Management of bleeding and procedures in patients on antiplatelet therapy. *Blood Rev.* 2020;39:100619. doi: 10.1016/j.blre.2019.100619

35. Durrant TN, van den Bosch MT, Hers I. Integrin alphaIIbbeta3 outside-in signaling. *Blood.* 2017;130:1607–1619. doi: 10.1182/blood-2017-03-773614

36. Tucker KL, Sage T, Gibbins JM. Clot retraction. *Methods Mol Biol.* 2012;788:101–107. doi: 10.1007/978-1-61779-307-3_8

37. Krafft MP, Riess JG. Therapeutic oxygen delivery by perfluorocarbon-based colloids. *Adv Colloid Interface Sci.* 2021;294:102407. doi: 10.1016/j.cis.2021.102407

38. Doshi N, Orje JN, Molins B, Smith JW, Mitragotri S, Ruggeri ZM. Platelet mimetic particles for targeting thrombi in flowing blood. *Adv Mater.* 2012;24:3864–3869. doi: 10.1002/adma.201200607

39. Huang G, Zhou Z, Srinivasan R, Penn MS, Kottke-Marchant K, Marchant RE, Gupta AS. Affinity manipulation of surface-conjugated RGD peptide to modulate binding of liposomes to activated platelets. *Biomaterials.* 2008;29:1676–1685. doi: 10.1016/j.biomaterials.2007.12.015

40. Haji-Valizadeh H, Modery-Pawlowski CL, Sen Gupta A. A factor VIII-derived peptide enables von Willebrand factor (VWF)-binding of artificial platelet nanoconstructs without interfering with VWF-adhesion of natural platelets. *Nanoscale.* 2014;6:4765–4773. doi: 10.1039/c3nr06400j

41. Sekhon UDS, Swingle K, Girish A, Luc N, de la Fuente M, Alvikas J, Haldeman S, Hassoune A, Shah K, Kim Y, et al. Platelet-mimicking procoagulant nanoparticles augment hemostasis in animal models of bleeding. *Sci Transl Med.* 2022;14:eabb8975. doi: 10.1126/scitranslmed.abb8975

42. Raghunathan S, Rayes J, Sen Gupta A. Platelet-inspired nanomedicine in hemostasis thrombosis and thromboinflammation. *Journal of thrombosis and haemostasis: JTH.* 2022;20:1535–1549. doi: 10.1111/jth.15734

43. Ohanian M, Cancelas JA, Davenport R, Pullarkat V, Hervig T, Broome C, Marek K, Kelly M, Gul Z, Rugg N, et al. Freeze-dried platelets are a promising alternative in bleeding thrombocytopenic patients with hematological malignancies. *Am J Hematol.* 2022;97:256–266. doi: 10.1002/ajh.26403

44. Leslie DC, Waterhouse A, Berthet JB, Valentin TM, Watters AL, Jain A, Kim P, Hatton BD, Nedder A, Donovan K, et al. A bioinspired omniphobic surface coating on medical devices prevents thrombosis and biofouling. *Nat Biotechnol.* 2014;32:1134–1140. doi: 10.1038/nbt.3020

45. Sato Y, Jinnouchi H, Kolodgie F, Cheng Q, Janifer C, Sakamoto A, Cornelissen A, Kawakami R, Mori M, Kawai K, et al. TCT CONNECT-250 comparison of thromboresistance of everolimus-eluting fluoropolymer stents and competitive drug-eluting stents between aspirin and clopidogrel single antiplatelet therapy using an ex vivo swine shunt model and evaluation of a novel flow loop model under aspirin single antiplatelet therapy. *J Am Coll Cardiol.* 2020;76:B110–B111. doi: 10.1016/j.jacc.2020.09.267

46. Slichter SJ, Pellham E, Bailey SL, Christoffel T, Gettinger I, Gaur L, Latchman Y, Nelson K, Bolgiano D. Leukofiltration plus pathogen reduction prevents alloimmune platelet refractoriness in a dog transfusion model. *Blood.* 2017;130:1052–1061. doi: 10.1182/blood-2016-07-726901

47. Ito Y, Nakamura S, Sugimoto N, Shigemori T, Kato Y, Ohno M, Sakuma S, Ito K, Kumon H, Hirose H, et al. Turbulence activates platelet biogenesis to enable clinical scale ex vivo production. *Cell.* 2018;174:636–648.e18. doi: 10.1016/j.cell.2018.06.011

48. Nakamura S, Takayama N, Hirata S, Seo H, Endo H, Ochi K, Fujita K, Koike T, Harimoto K, Dohda T, et al. Expandable megakaryocyte cell lines enable clinically applicable generation of platelets from human induced pluripotent stem cells. *Cell stem cell.* 2014;14:535–548. doi: 10.1016/j.stem.2014.01.011

49. Hu CM, Fang RH, Wang KC, Luk BT, Thamphiwatana S, Dehaini D, Nguyen P, Angsantikul P, Wen CH, Kroll AV, et al. Nanoparticle biointerfacing by platelet membrane cloaking. *Nature.* 2015;526:118–121. doi: 10.1038/nature15373